Research Journal of Engineering Sciences E- ISSN 2278 – 9472
Vol. **5(5),** 20-30, May **(2016)** *Res. J. Engineering Sci.*

Experimental research on Aerodynamic Performance of an USPLSC airfoil

Yadav Khagendra Kumar
School of Aeronautics, Northwestern Polytechnical University, Xi`an, China
khagendrakryadav@gmail.com

Available online at: www.isca.in, www.isca.me
Received 3rd March 2016, revised 26th April 2016, accepted 24th May 2016

Abstract

Fre-and-aft symmetrical upper surface protrude lower surface concave (USPLSC) airfoils have been developed for the coaxial rotating wing of an UAV. In order to understand the aerodynamical performance of the airfoil, low speed wind tunnel experiment is carried out to measure lift coefficient, drag coefficient and pressure distribution under wind speed 20~40 m/s. Results are compared with CFD prediction using Fluent software. A satisfied agreement has been achieved and error analysis is provided. The purpose of this study is to conduct a parametric investigation on the performance of USPLSC airfoils for coaxial rotating wing UAV. The main objective of this study is to test USPLSC in wind tunnel and compare the experiment result with CFD simulation result.

Keywords: Airfoil, UAV, Wind tunnel experiment, CFD.

Introduction

The USPLSC Project is a 2 years research project at Northwestern Polytechnical University (NWPU), China, which is focused on in coaxial rotor wing UAVs to obtain vertical takeoff and landing. Fixed wing UAVs have the disadvantage of requiring runway or launcher for takeoff-landing and not being able to hover. On the other hand, rotary wing UAVs have the advantage of being able to hover, takeoff and land vertically with agile maneuvering capability at the expense of high mechanical complexity.

There are many studies on rotorcraft UAVs with different rotor configurations. In this thesis attention is paid to configure the wing by one USPLSC airfoil, working likes a rotating blade. The design of the fixed wing UAV conversion into the rotor wing UAV modifications remained the basis of the original aerodynamic design. Second part presents a brief survey of airfoils. Third part presents wind tunnel equipment and experiment. At last the CFD simulation and result compare with experiment.

General discussion of UAVs: From the mid-1960s the use of UAVs for intelligence, surveillance and reconnaissance (ISR) mission has featured in operations over Chechnya, China, the Middle East, South-East Asia and the former Yugoslavia. Currently, more than three dozen nations are active in developing UAV technology, and the leader in advancements of UAV technology is the US. Over five dozen different programs including the American Predator, Global Hawk and Shadow make up the United States' arsenal of UAV.

In recent years, interest has grown in using UAVs predominantly for military applications, but also used in a small but growing number of civil applications, such as policing, firefighting, and nonmilitary security work, such as surveillance of pipelines. UAVs are often preferred for missions that are too "dull, dirty, or dangerous" for manned aircraft. For this reason, there is an increasing demand for these vehicles in civilian and military applications. In addition, advancements in unmanned technology allow UAVs to be less expensive, higher performing, and more maneuverable.

UAV model: The ASN-206 shown in Figure-1 is a twin boom, lightweight, short-range, tactical multi-purpose UAV. The presented UAV can be used for day/night aerial reconnaissance, countermeasures (EW/ECM), electronic warfare and battlefield surveillance, target location, spotting of ordnance and tanks, to keep eye on border, aerial photography and for searching mineral deposits, and to find out the aircraft in sky. It is the most popular and advanced tactical UAV systems fielded by the PLA. A unique designed the ASN-206 are fitted or can be fitted with various equipment according to the requirements. The most usable and very important feature about ASN-206 is the real-time video images transferring system to the ground control, while older-generation UAVs have to be bring down before the photo and video can be retreated.

The UAV is being widely used as it's the most economical and multifunction. The ASN-206 has propeller mounted on tail, which is used as tail-pushed. The beneficial of using tail-mounted propeller engine is that the propeller will not disturb the sight of reconnaissance system.

The ASN-206 is capable of mounting with different types of high range cameras or television operator for real time broadcasting. The navigation systems of the UAV incorporate GPS and radio command. The original UAV (ASN-206) studied

in this thesis has a traditional overall aero dynamical design. ASN-206 specification is: Wingspan (m): 6, Length (m): 3.8, Height (m): 1.4, Weight (m): 222, Payload (m): 50 max, Max speed (km/hr): 210, Range (km): 150

Figure -1
Original design of the UAV

Brief introduction of coaxial counter rotating wing: This thesis aims to modify UAV ASN-206 with coaxial counter rotating wing (CCRW), as shown in Figure-2. The aim is to produce a UAV that will be able to realize self-take off, landing and hovering without significant change of the aerodynamical design of the overall plane. This preliminary design effort will assist in future development of an UAV which will have the following advantages 1) self-takeoff and landing; 2) hovering capability and high efficiency since there is no tail rotor and therefore do not need to balance the rotor torque and power consumption; 3) aerodynamic symmetry; 4) vertical and horizontal control efficiency; 5) compact structure, weight and high efficiency; 6) have a greater rate of climb and service ceiling. Therefore rotary wing coaxially reverse rotation design, the anti-torque of the propeller of the aircraft is not only eliminated, eliminating the tail rotor, and improve the propeller efficiency and stability[1].

The rotating wing has no twist angle. It is installed to the suitable angle. Additional engine and control system need to be employed for the UAV. Some coaxial helicopter techniques are involved, but not to the complicated extent. For example, in forward fly, rotating wing only works before transition period.

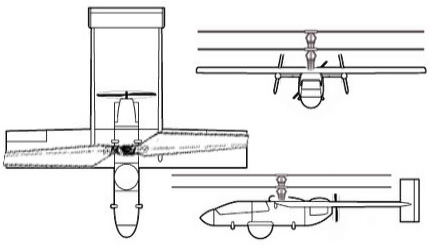

Figure -2
UAV ASN-206 with CCRW

For cruise condition, the CCRW will be fixed to provide additional lift. For the transition period, the original wing and tail can provide lift, while CCRW decreases and locked in the same direction of the original wing. Soon after that a pitch control device will be employed to change left top and right bottom wing pitch angle in a small range (5~10°). As a consequence, a rotating wing changes to a fixed wing. The USPLSC airfoil is designed specifically for the CCRW. Because USPLSC airfoil shape is symmetrical to the middle chord position, it requires a smaller range of pitch angle for transition from rotating into a fixed wing than traditional airfoil (90~180°).Other control system remains same as the basic fixed-wing control system[2].

Aerodynamics of airfoils and Wind tunnel test

In this section the aerodynamics of airfoils are discussed as well as the testing of proposed airfoil with wind tunnel.

Airfoil: The aircraft is lifted by its wing. The wing has a finite length called wing span. If the wing is sliced with a plane parallel to the x-z plane of the aircraft, the intersection of the wing surfaces with that plane is called an airfoil having the function of producing a controllable net aerodynamic force by its motion through the air[3]. To be useful this aerodynamic force must have a lifting component that is much greater than the resistance or drag component. In a powered aircraft, motion through the air is provided by the thrust; so in effect, the airfoil is a device that converts thrust into lift; in a glider the airfoil converts much of the gravitational force (the potential energy of height) into lift.

Aerodynamic forces: The aerodynamics force is the resultant of all forces on a profile in airflow acting on the center of the pressure. The aerodynamic force has two components lift, which is perpendicular to the relative wind, and drag, which is parallel to the relative wind. Here the center of pressure is identified. This is the point on which all pressures and all forces act. This point is located where the cord of a profile intersects with the resultant of the aerodynamic forces lift and drag. This point is expressed as a percentage of the chord of the airfoil. A center of pressure at 30 percent of a 60-inch chord would be 18 inches aft of the wing's leading edge. The aerodynamic forces of the lift and drag depend on the combined effect of the many variables-the dynamic pressure the surface area of the profile the shape of the profile and the angle of the attack (The angle at which the chord c of the airfoil moves in relation to the free stream is known as the angle of attack)[4].

Velocity and pressure distributions: Velocity and pressure are dependent on each other - Bernoulli's equation says that increasing the velocity decreases the local pressure and vice versa. Thus the upper surface static pressure in less than ambient pressure, while the lower surface static pressure is higher than ambient pressure. Ambient pressure is pressure of the surrounding medium, which comes into contact with the object. This is due higher airspeed (velocity) at upper surface

and lower speed at lower surface of the airfoil. It is possible to plot a pressure distribution instead of the velocity distribution (usually not the pressure, but the ratio of the local pressure to the stagnation pressure is plotted and called pressure coefficient

Cp): $c_p = \frac{p - P_\infty}{\frac{1}{2} \cdot V_\infty^2}$ 1

Where: P - Static pressure at the point of interest, P∞ - Free stream static pressure, v∞ - Free stream velocity, ρ - Free stream density

USPLSC airfoil: The geometry of USPLC airfoil is shown in Figure-3, it is a new airfoil designed with blunt leading and trailing edge. The USPLC airfoil is a thin, curved airfoil which can improve the aerodynamic characteristics in VTOL. The upper surface is protruded and the lower surface is concave. This is basically to design for the coaxial rotor wing UAV, to get the vertical takeoff and landing (VTOL). The camber distribution and thickness distribution are shown in the Figure-4 and 5. Maximum thickness of the airfoil is 10% and the max camber is 12% at the 50% of the chord length. The radius on the leading and trailing edge is 1.48/100 of the chord length.

Figure-3
Geometry of USPLSC airfoil

Figure-4
Geometry of USPLSC airfoil

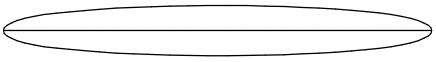

Figure-5
Thickness distribution of USPLSC airfoil

As can be seen the both leading and trailing edges are blunt, having the same radius for both edges. While the maximum camber ratio is almost in the middle of the airfoil. Having the maximum camber ratio in the middle of the airfoil causes the small lift coefficient, while the drag coefficient is bigger, the blunt trailing edge may bring vortex problem.

Both leading and trailing edges are blunt so the stall angle will be smaller, because the drag will be greater than the other conventional airfoil's case. To get the cl, cd, cl/cd, and vortex problem showed by CFD simulations.

Airfoil pressure measurement: The experiment helps to obtain pressure distribution on the airfoil and compute the lift and drag coefficient at different angle of attack at 3 working conditions (20m/s, 30m/s and 40m/s). Experiment equipment are explained below.

Wind tunnel: The experiment is carried out in the LTWT in North-western Polytechnical University. It is a low-speed wind tunnel (the air is drawn directly from the surroundings into the wind tunnel and rejected back into the surroundings). It is 39.52 meters long, structured by steel.

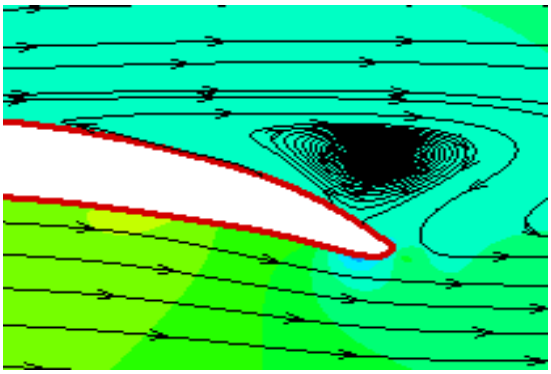

Figure-6
Vortex structure of USPLSC airfoil at Mach 0.4, AOA = 5°

There are two available replacement test section: 3D and 2D test section. This paper tests in the 2D test section, Test section dimensions: length × width × height = 3.2 × 1 × 0.4m, Ma = 0.015 ~~ 0.22., 3D test section： 1.05×1.2 m， V = 5 ～ 55 m/s, 3D test section (3D and 2D serial status)： 1.05×1.2 m, V = 5 ～ 25 m/s, 2D test section：0.4 ×1.0 m， V = 5～ 75 m/s, Minimum turbulence level： ε＜ 0.02%, Turbulence level changing range：0.02% ～ 1%

Airfoil Model material and pressure taps: The model is made up by paulownia wood. The pressure distribution around the airfoil is obtained from 60 pressure taps (small holes drilled perpendicular to the surface of the blade). The outer/inner diameter of the copper pipe is 1.2/0.7mm. The pressure taps were placed along the upper and lower surface at the middle of the span in a staggered alignment to minimize disturbances from upstream taps. The taps were drilled directly through the model surface and into copper tubes lying parallel to the model surface. Pressure tubes (tygon tubes) were connected to the copper tubes and they were lead outside and connected the scanning valve that sequentially cycles through each pressure tap.

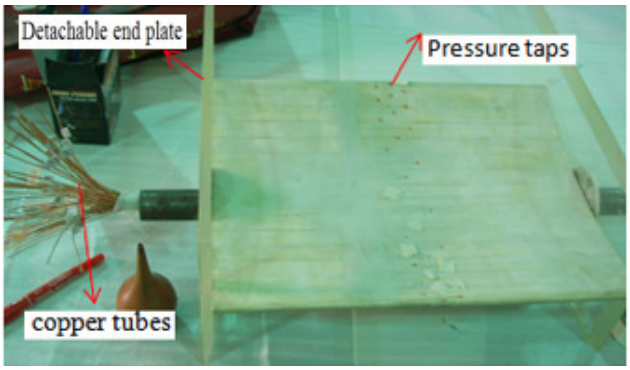

Figure-7
Airfoil section shape and pressure taps arrangements

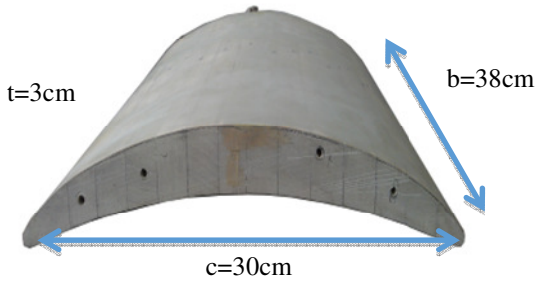

Figure-8
Airfoil model

Pitot rake: To measure the drag of the airfoil, a pitot rake is employed. It consists of 120 total pressure probes and 4 static pressure measure tubes, height: 300 mm. It placed back on the airfoil with distance of 0.5 ~ 1 chord lengths to the trailing edge of the airfoil. Pitot rake is perpendicular to the wind tunnel axial direction; it allows the simultaneous measurements of velocity across the wake.

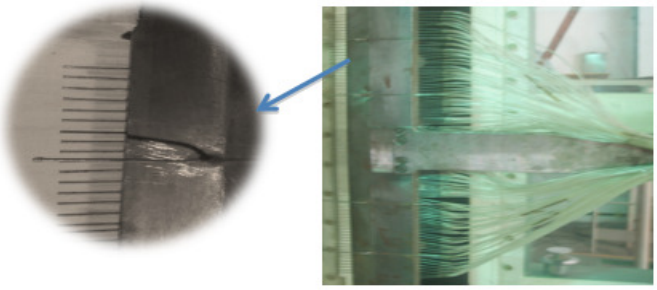

Figure-9
Pitot rake

Airfoil pitch control: The angle of attack of the airfoil in the wind tunnel test section is change using a computer controlled pitching system that can rotate the airfoil through a full 360°. A motor drives the pitching system, Figure -10.

Figure-10
Airfoil pitch controller

Pressure measuring system: The measuring system employs DSY104 electronic scanning micro pressure measuring system, manufactured by NWPU. Pressure measuring channel: 192 channels, （± 2.5kPa 160 channels，± 7.5kPa 32 channels) Canning rate: 50000 channel/s. System precision：± 0.1％F.S

Test section: 2D test section is employed to carry out the experiment, is explained. The wall-mounted airfoil and setup is shown in Figure -11 and 12.

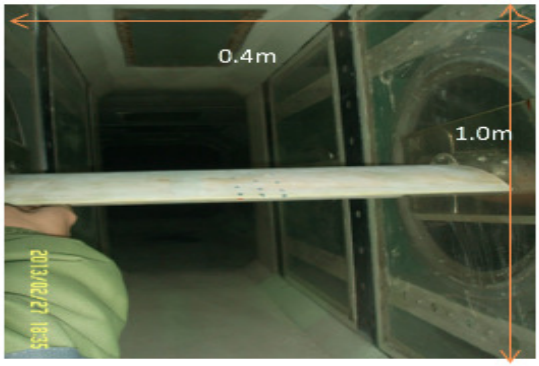

Figure-11
Wall-mounted airfoil in test section

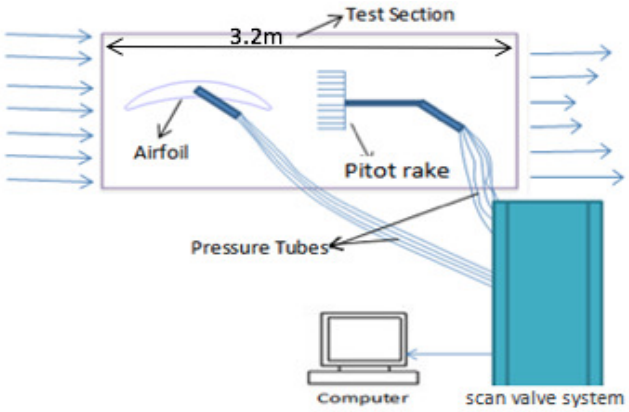

Figure-12
Test section

Experiment status: The wind tunnel experiments are taken at different working condition mention in Table-1.

Table-1
Working conditions for the experiment

V (m/s)	Re	Angle of attack (α°)
20	4.11×105	-2,0, 2, 4, 6, 8, 10, 12, 14
30	6.16×105	-2,0, 2, 4, 6, 8, 10, 12, 14
40	8.22×105	-2,0, 2, 4, 6, 8, 10, 12, 14

Experimental result and analysis: The curve of the lift and drag coefficients versus the angle of attack are presented below.

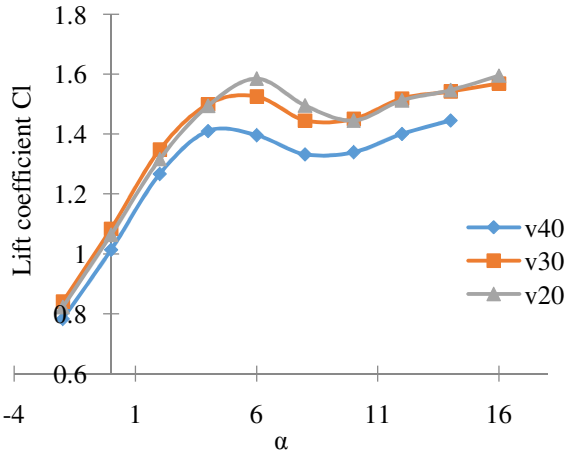

Figure-13
c_l at various angles of attack from experimental data

As it can be seen from Figure-13, the results show a relationship between the coefficient of lift and angle of attack. When AOA increases from 0° to 6°, c_l increases to maximum value 1.4~1.6. When AOA increases from 6° to 10°, c_l decreases a little bit and increases when AOA increases from 10° to 16°.

Figure-14 shows that the minimum c_d is obtained when AOA is in 2 to 4°, the min c_d is 0.02~0.03. c_d Increases when AOA increases from 4 to 16°.

Lift increases proportionately with respect to the angle of attack and wind speed, up to the critical angle of attack 6°. Lift coefficient do vary with wind speed. These coefficients are useful to analyse airfoils at different wind speed without performing a wind tunnel analysis for each wind speed.

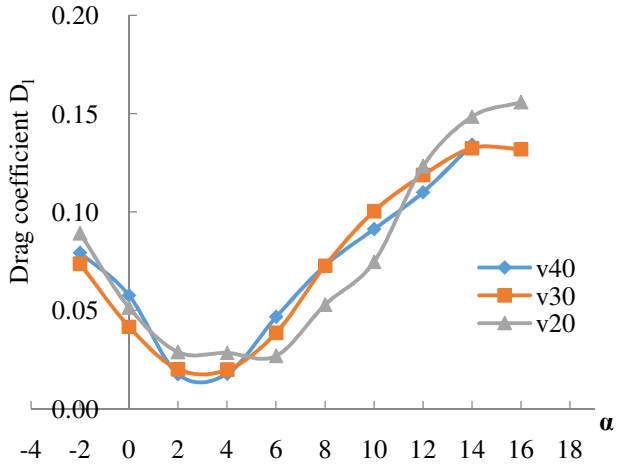

Figure-14
c_d at various angles of attack from experimental data

Table-2
Experimental c_l, c_d vs AOA results for V=20~40m/s

	Value	AOA
$c_{l,max}$	1.4~1.6	6° ~ 10°
$c_{d,min}$	0.02~0.03	2°~ 4°
Stall	c_l =1.4~1.6	6°(smooth stall)
Optimum AOA	c_l=1.3~1.5, $\frac{c_l}{c_d}$= 59~79	4°~6°

It can be concluded that the optimum angle of attack is between 4-6°at different velocity condition. The reason is that at this range the ratio between the coefficient of lift and the angle of attack is at its maximum. As a result, it is reasonable to assume that in order to obtain maximum lift from USPLS Cairfoil, the wing needs to be positioned at 4-6 degrees with respect to the flight path.

Pressure distributions curves for the USPLSC airfoil airfoils are shown in chapter IV with comparison of CFD.

Error analysis: Every contribution to the flow of the data stream from sensor to reported data is a source of uncertainty in the final product. In general, the sources of error can be classified as test technique, model, tunnel, instrumentation, and math model related.

Errors of the experiments come from model shape, wind velocity error, angle of attack and pressure measuring system. Each one is explained in details:

Model shape: As it explained before the model is made up by paulownia wood. When the model is fully made, it slowly contracts when the air is dry and changes shape about some millimeters, which results in error while experiment process.

Pressure tap: The error can be due to the variations in local tap geometry and the second reason may be the roughness near the taphole. Examples of poor design as well as the proper design of the pressure tabs are shown in Figure-15. Ideally, to achieve low error, the pressure tap hole need to have a certain geometry as illustrated in Figure-20, (b) with a smooth surface around the hole and perpendicular to the wall. In this case the static pressure reading is equal to P∞.

The assumption can be made that the streamlines are parallel to the tap surface. In a) lower pressure than P∞ is read as a result; In c) added roughness can cause the flow to slowdown in the tap region resulting in a pressure reading greater than P∞ In d) have a similar effect as the roughness.

Wind velocity error

Velocity fluctuation: Both the velocity fluctuation and turbulence of the wind tunnel will result in error. For low speed experiment, it is difficult to control the velocity at test section to be steady. Because the rotating velocity of the blowing fan controls speed, it is difficult to maintain the rotating speed at a low value, i.e. any oscillation of the rotating speed will result in a relative wind velocity, which cannot be ignored.

Turbulence: Although the LTWT has a small value of turbulence(Minimum turbulence level : $\varepsilon < 0.02\%$), it will influences the error. If turbulence value can be decreased, then error will be decreased.

Angle of attacks: An airfoil pitch control shown in figure no-15 can cause error. Motor drives inside an airfoil pitch controller device change the AOA. While changing AOA it doesn't give a high accurate AOA. For example AOA 8° it can change the airfoil to AOA 7.8° or 8.1°.

Pressure measuring system:DSY104 electronic scanning micro pressure measuring system is employed to measure pressure distribution, whichhas a certain level of error.

CFD simulations

This simulation of flow passing the airfoil is performed, using computational fluid dynamics (CFD) software Fluent. CFD results of the surface pressure distribution, lift and drag force acting on the airfoil are compared with experimental data. The simulation been has developed after the laboratory experiment and therefore we use the same USPLSC airfoil geometry as well as the same flow parameters, such as fluid density, viscosity, angle of attack, and free stream velocity.

CFD is the analysis of systems involving fluid flow, heat transfer and associated phenomena such as chemical reactions by means of computer-based simulation. The technique is very powerful and spans a wide range of industrial and non-industrial application areas. CFD codes are structured around the numerical algorithms that can tackle fluid flow problems. In order to provide easy access to their solving power all commercial CFD packages include sophisticated user interfaces to input problem parameters and to examine the results. Hence all codes contain three main elements: (i) a pre-processor, (ii) a solver and (iii) a post-processor[5].

In the fluid dynamics, there are many commercial CFD packages available for modeling flow in or around objects. The computer simulations show features and details that are difficult, expensive or impossible to measure or visualize experimentally. The simulation is performed on the commercial CFD code Fluent. Figure no 16 shows the structure of Fluent software, where pre-processing is completed in software[6]. Gambit is a mesh generator[7]. First, Gambit is used to make a discretization of flow domain, and then Fluent is applied to solve the flow.

CFD simulation of USPLSC airfoil: CFD simulation of USPLSC airfoil is done by Gambit and Fluent. Mesh is generated by software Gridgen then imported to Gambit. The mesh contains 80,000 cells, circulation division × radial division is 400×200. Then use the Fluent solver is used to get results for USPLSC airfoil at various angle of attack and Mach numbers.

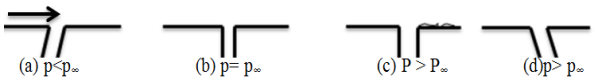

Figure-15
Schematic of pressure tabs. (a), (c) and (d) poor design. (b) Proper design

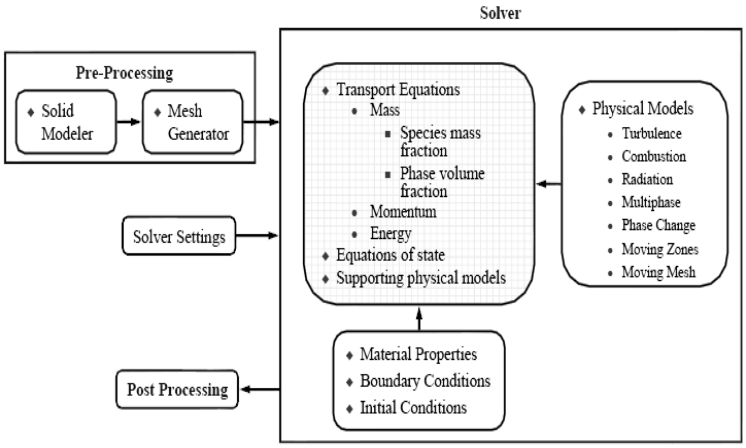

Figure-16
The composition of the CFD solver

The global mesh for USPLSC airfoil is shown in Figure-17 below. Figure-18 below shows the local mesh distribution for USPLSC airfoil.

Working conditions: The CFD simulation is completed over velocity 20 to 40m/s. Next section below show the some graph along with experiment result. Nest Section only represents the graph at velocity 20m/s.

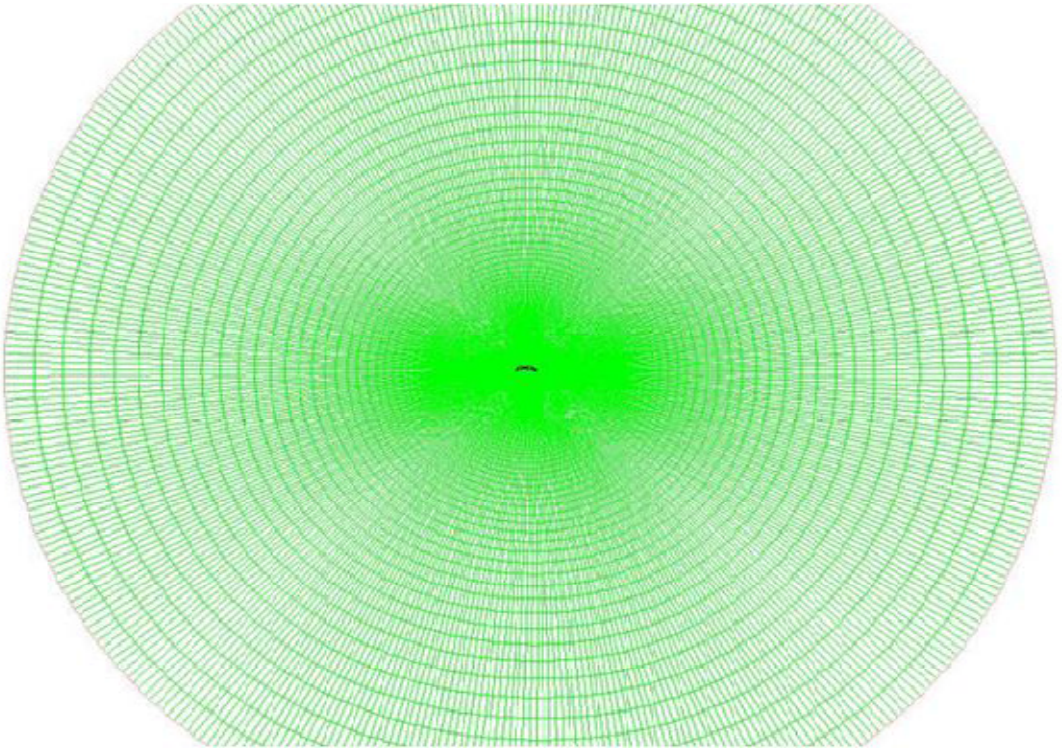

Figure-17
Global mesh distribution of USPLSC airfoil

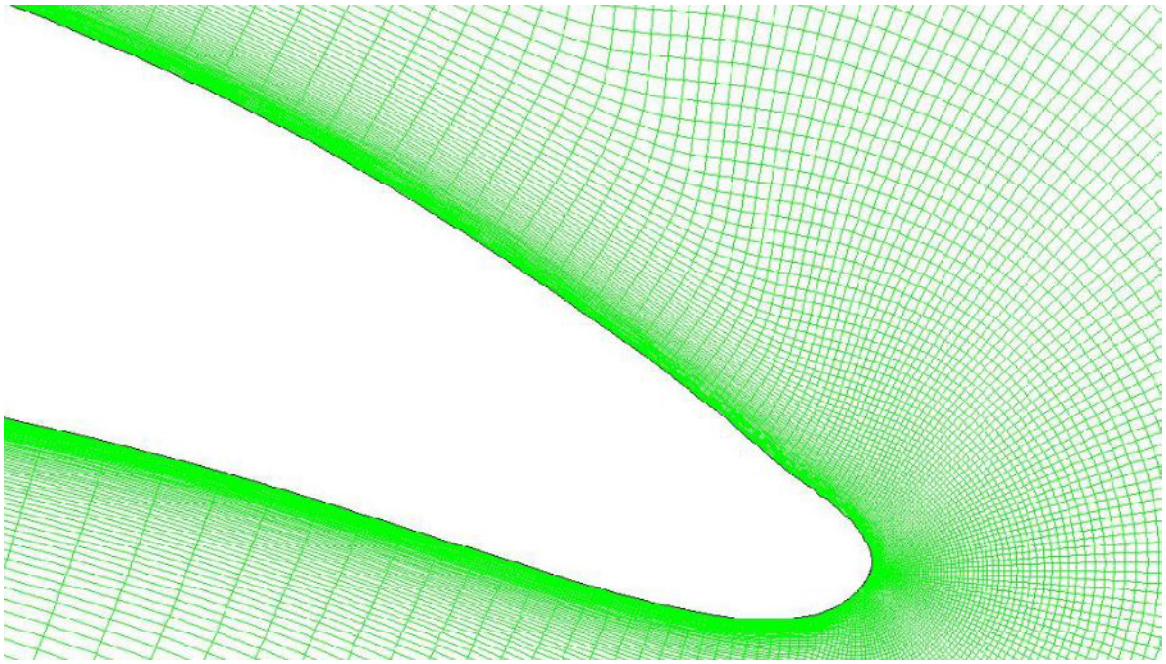

Figure-18
Local mesh distribution for USPLSC airfoil

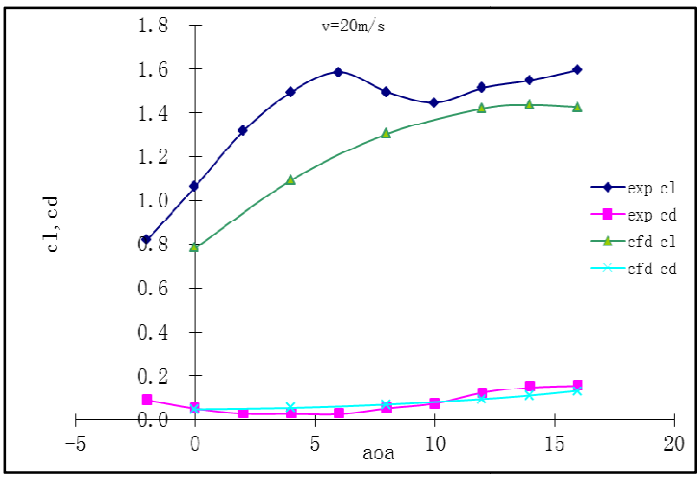

Figure -19
c_l, $c_d$varying AOA at v=20m/s

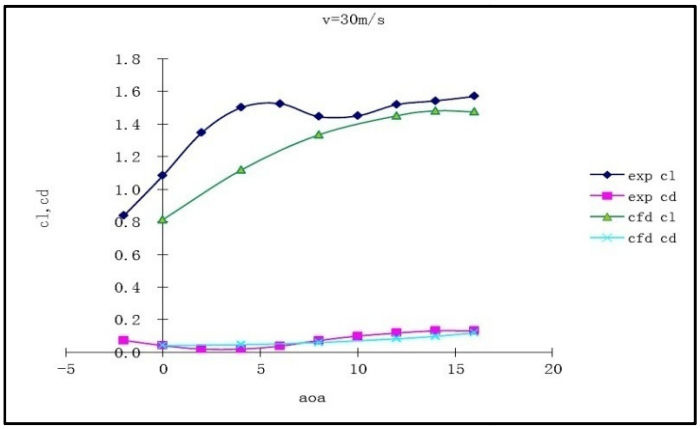

Figure-20
c_l, $c_d$varying AOA at v=30m/s

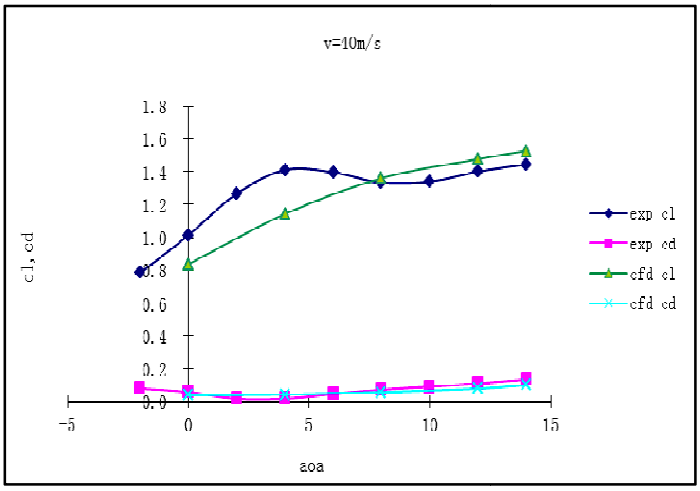

Figure-21
c_l, $c_d$varying AOA at v=40m/s

Comparison of c_l, c_d: From these three graphs it can be observed that the agreement between experiment and CFD C_d is satisfied. The comparison between experiment and CFD C_l is good above 7.5° AOA. Below 7.5° AOA the k-e prediction is maximum difference of C_l. The CFD error of c_l is -27~-6% compared with experimental result (for v=20m/s).

Comparison of C_P: Comparison of pressure distributions at various AOA for the USPLSC airfoil is shown below.

There is some scatter in the C_P values at the top of the airfoil near leading edge region until x/c = 0.17, caused by either uncertainty of the calibration or small irregularities of the surface or the pressure taps.

As can be seen from Figure-22 to 25 when AOA increases C_p difference between experiment and CFD decreases. This is the reason why c_l difference is small at high AOA between experiment and CFDthan small AOA.

In order to understand the static pressure distribution and streamline across the airfoil, Figure-26 to 29 present the results from CFD calculations. As can been seen from Figure-26 to 29, there is a flow separation at the rear of the upper surface. The pressure distribution of the airfoil is high pressure at lower surface and low pressure at upper surface.

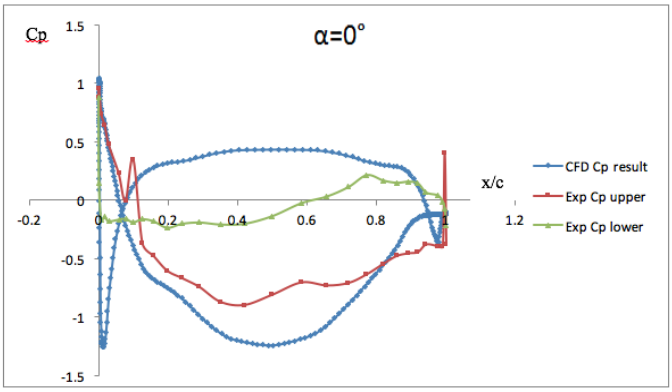

Figure-22
c_p comparison at AOA=0^0

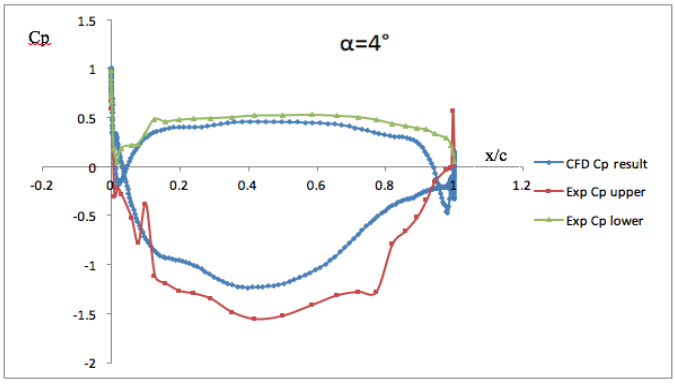

Figure-23
c_p comparison at AOA=4°

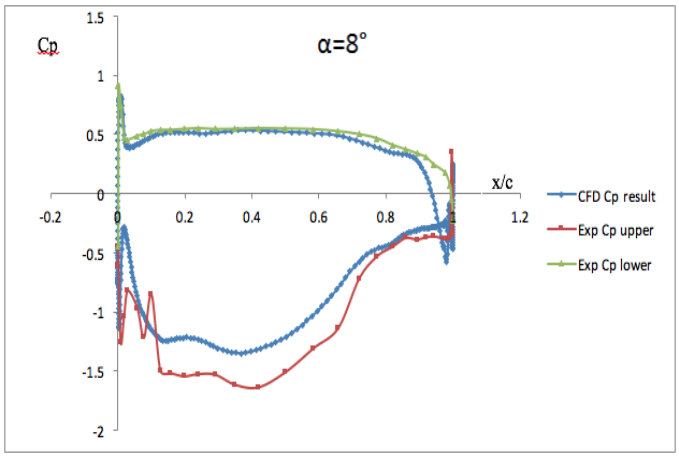

Figure-24
c_p comparison at AOA=8^0

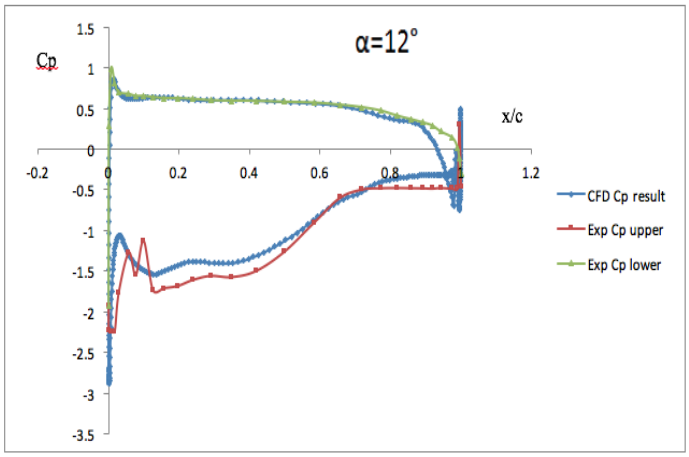

Figure-25
c_p comparison at AOA=12^0

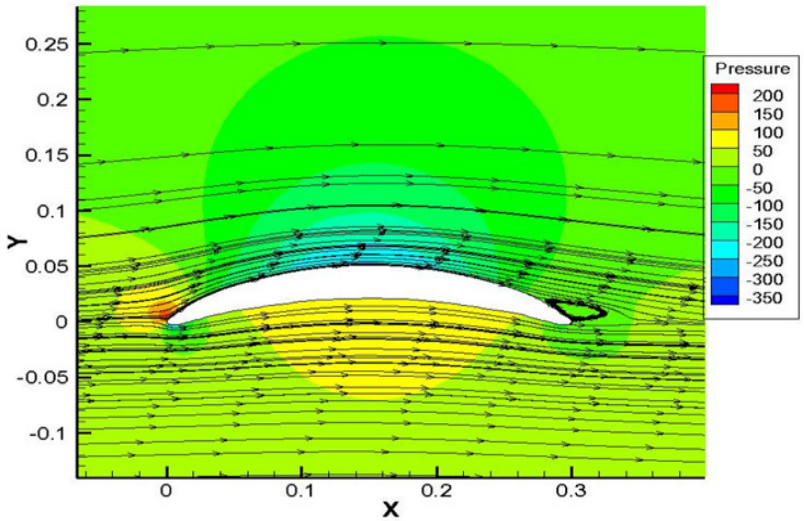

Figure-26
Static pressure distribution (Pa) and streamline for AOA=0° at v=20m/s

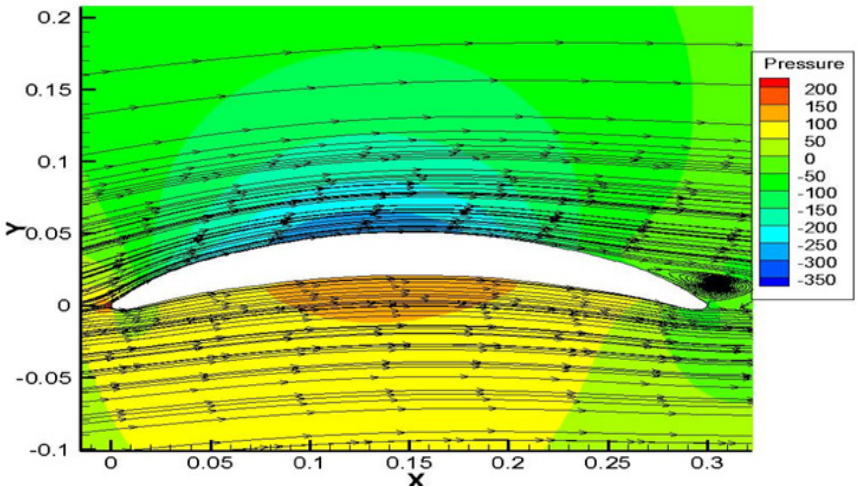

Figure-27
Static pressure distribution (Pa) and streamline for AOA=4° at v=20m/s

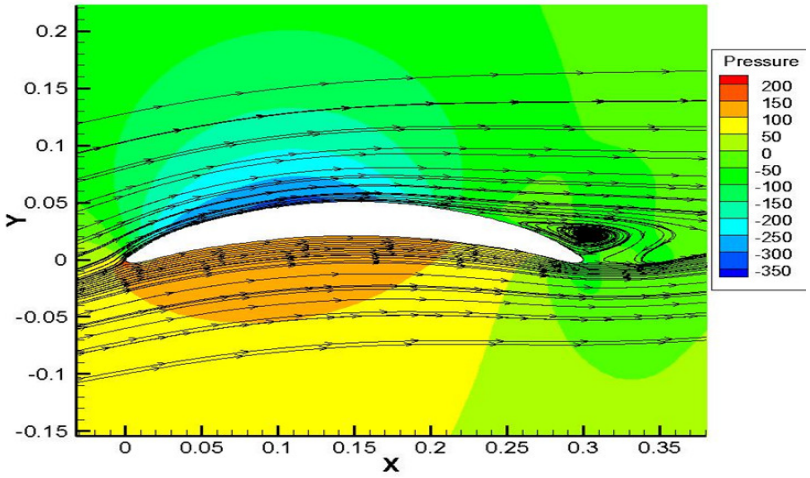

Figure-28
Static pressure distribution (Pa) and streamline for AOA=8°at v=20m/s

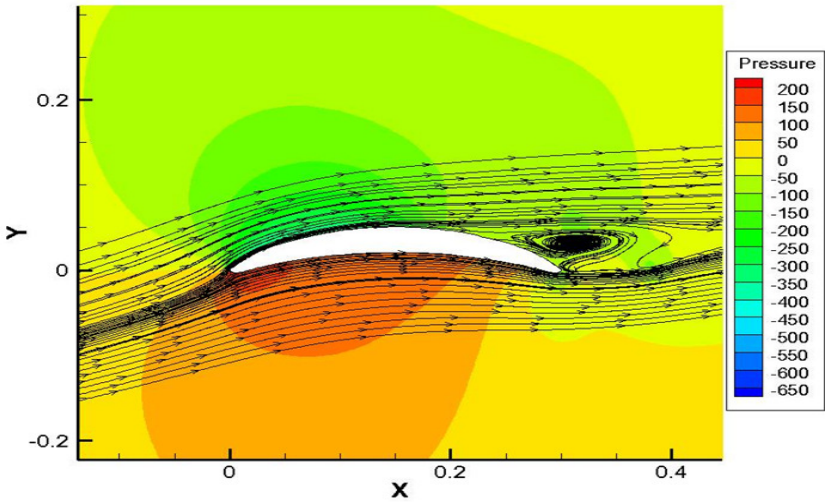

Figure-29
Static pressure distribution (Pa) and streamline for AOA=12°at v=20m/s

Conclusion

In this thesis it has been studied to improve in UAV technology, primarily the CCRWUAV concept, resulted in the conclusion that a parametric study into the aerodynamic performance of fre-and-aft symmetrical USPLSC airfoils would benefit future research in CCRW technology development and could serve as a tool for new coaxial rotor-wing design concepts.

Wind tunnel tests with approximately 2D flow were carried out for the USPLS Cairfoil in the LTWT wind tunnel binary test section at velocity 20~40m/s to obtain the airfoil surface pressure distribution data. To predict the aerodynamic performance at the each part of the wing, 3 different working conditions are employed. Each condition has one precise velocity and 9 different AOA. The result obtains from wind tunnel showed that the airfoil behaved well according to the design assumptions. In order to obtain maximum lift from USPLS Cairfoil, the wing needs to be positioned at 4-6º with respect to the flight path. The curve of the lift coefficient versus the angle of attack shows a stall at 6º. The stall is smooth.

CFD simulation has performed over 2D USPLSC airfoil. Comparisons between experiment and CFD simulation result were carried out with the USPLSC airfoil. The comparisons were in good agreement with their results. The result shows when AOA increase the Cp difference between experiment and CFD decrease. This is the reason why c_l, difference is small at high AOA between Experiment and CFD. The CFD error of cl is -27~-6% compared with experiment result for v=20m/s.

Acknowledgment

I express my deepest gratitude to Associate Professor Zhao Xu for making this work possible.

Future work: To understand the more detail about the airfoil, it need to perform high speed wind tunnel experiment 50~100m/s. In the main, refinement of model and measurement technology improvements in wind tunnel.

Investigation on CFD error analysis and improvement in the development of airfoil model. A more complete grid convergence study and a further validation study would both need to be conducted to develop better techniques and methodology for aerodynamic USPLSC analysis of airfoils.

References

1. Gordon Leishman J. (2000). Principles of Helicopter Aerodynamics with CD Extra. Cambridge University Press, New York, 1-4. ISBN: 987-0-521-66060-0.

2. Colin P. Coleman. (1997). A survey of theoretical and experimental coaxial rotoraero dynamic research. Ames Research Center, Moffett Field, California. 0704-0188

3. John D. Anderson Jr. (2005). Fundamentals of aerodynamics. McGraw-Hill Education, ISBN-13: 978-0073398105

4. Emami M.R. (2007). Aerodynamic forces on an airfoil. AER 303F, Aerospace Laboratory I. University of Toronto, Toronto.

5. Chow, C.Y. (1979). An introduction to computational fluid dynamics. John Wiley and Sons, Inc.,New York, NY

6. FLUENT 6.3. (2006). User Guide, FLUENT Inc. of American.

7. GAMBIT 6.2. (2006). User Guide, FLUENT Inc. of American.